

## Rotational mobility of $\text{Ca}^{2+}$ -ATPase of sarcoplasmic reticulum in viscous media

Marianna Török <sup>a,b</sup>, Györgyi Jakab <sup>a</sup>, Alajos Bérczi <sup>b</sup>, László Dux <sup>a</sup>, László I. Horváth <sup>b,\*</sup>

<sup>a</sup> Department of Biochemistry, Szent-Györgyi Albert Medical School, Szeged, Hungary

<sup>b</sup> Institute of Biophysics, Biological Research Centre, Temesvári krt 62, P.O. Box 521, H-6701 Szeged, Hungary

Received 8 November 1996; revised 24 January 1997; accepted 31 January 1997

---

### Abstract

The rotational diffusion of  $\text{Ca}^{2+}$ -ATPase [ $\text{Ca}^{2+}$ ,  $\text{Mg}^{2+}$ -activated ATP phosphohydrolase E.C. 3.6.1.38] was studied in native sarcoplasmic reticulum membrane by saturation transfer ESR spectroscopy after covalent labelling of intramembraneous sulfhydryl groups with nitroxyl derivative of maleimide (5-MSL) as a function of sucrose and glycerol in the suspending medium. The relative enzymatic activity of sarcoplasmic reticulum was followed by increasing the viscosity of the aqueous phase. The ATP hydrolysing activity of the enzyme decreased differently on adding sucrose and glycerol. In the case of sucrose the reciprocal of power dependence of viscosity was observed, whereas for glycerol an exponential decay law was obtained, indicating solvent-protein interaction. On increasing the viscosity of the aqueous phase by either sucrose or glycerol, no changes were observed in the intramembraneous viscosity as measured using intercalated spin-labelled stearic acid (16-SASL). The effective rotational correlation time of the protein was measured, as a mobility parameter, using saturation transfer ESR spectroscopy and found to be increased linearly with the viscosity of the sucrose containing medium and for the extramembraneous size a height of 6.8 nm was obtained, indicating that approx. 82% of the volume of  $\text{Ca}^{2+}$ -ATPase protein is external to the sarcoplasmic reticulum. The addition of glycerol probably promoted protein–protein interaction, as indicated by the larger changes in rotational diffusion and non-linear viscosity dependence.

**Keywords:** Rotational mobility;  $\text{Ca}^{2+}$ -ATPase; Saturation transfer ESR; Viscosity dependence

---

### 1. Introduction

The overall molecular mobility of transmembrane proteins is driven by the intramembraneous frictional torque in the viscous hydrophobic phase unless the frictional forces in the aqueous phase are significantly increased by adding polyols to the suspending medium [1,2]. The effect of increasing viscosity in the aqueous phase depends on the relative sizes of the extramembraneous-to-intramembraneous parts of proteins.  $\text{Ca}^{2+}$ -ATPase of sarcoplasmic reticulum is an appropriate representative of numerous proteins with

---

Abbreviations: SR, sarcoplasmic reticulum; ESR, electron spin resonance; STESR, saturation transfer electron spin resonance; EM, electron microscopy; EGTA, ethylene glycol bis( $\beta$ -aminoethyl ether)-N,N,N',N'-tetraacetic acid; MOPS, 3-(N-morpholino)propanesulfonic acid; NEM, N-ethylmaleimide; 5-MSL, 3-maleimido-1-oxyl-2,2,5,5-tetramethylpyrrolidine; 16-SASL, 16-(N-oxy-4',4'-dimethyloxazolidin-2-yl) stearic acid

\* Corresponding author. Fax: +36 62 433133.  
E-mail: horvathl@everx.szbk.u-szeged.hu

voluminous extramembranous protrusions [3,4]. Clearly, molecular size data can be determined by rotational measurements provided the addition of polyols does not introduce large-scale conformational changes in the protein [5]. The mobility of integral membrane proteins is low; typical correlation times are in the range of  $10^{-6}$  to  $10^{-4}$  s. In such instant saturation transfer ESR (STESR) spectroscopy [6–8] is a suitable technique for quantitative measurements of rotational mobility and, hence, hydrodynamic sizes using covalently attached nitroxyl spin labels.

In this work the viscosity of the aqueous phase was increased by adding sucrose or glycerol and the rotational rate of  $\text{Ca}^{2+}$ -ATPase of sarcoplasmic reticulum (SR) was measured by STESR spectroscopy using covalently attached spin labelled maleimide (5-MSL) at low labelling level ( $\text{MSL}_{\text{bound}}/\text{Ca}^{2+}\text{-ATPase} = 0.75$  mol/mol). The effect of polyols on the intramembranous viscosity was followed by intercalated lipid spin labels, using C-16 stearic acid spin probes (16-SASL). In a parallel set of experiments the effect of polyols on the relative enzymatic activity of the enzyme was followed. From hydrodynamic data the size of the extramembranous domains protruding to the aqueous phase was determined.

## 2. Experimental procedures

### 2.1. Materials

Sucrose and glycerol were of analytical grade purity from Serva (Heidelberg, Germany) and Sigma (Munich, Germany), respectively. Spin labelled maleimide (5-MSL) and C-16 labelled stearic acid (16-SASL) were from Sigma (Munich, Germany) and N-ethylmaleimide (NEM) was from Serva (Heidelberg, Germany), dissolved in dimethylsulfoxide (DMSO, Sigma-Aldrich, Munich, Germany).

Sarcoplasmic reticulum vesicles were prepared as described by Nakamura et al. [9] from rabbit skeletal muscle. In the enzymatic activity and crystallization experiments the following solutions were used 0.1 M KCl, 10 mM MOPS (pH 7.4), 5 mM  $\text{MgCl}_2$ , 0.5 mM EGTA (Medium S) and 0.1 M KCl, 10 mM imidazole (pH 7.4), 5 mM  $\text{MgCl}_2$ , 0.5 mM EGTA (Medium C) with 5 mM decavanadate, respectively. Viscosity of Medium S mixtures supplemented with sucrose or

glycerol was measured with a thermostated rotating disc viscometer at 298 K (Haake, Germany).

### 2.2. Enzymatic activity measurements and negative staining electron microscopy

$\text{Ca}^{2+}$ ,  $\text{Mg}^{2+}$ -activated ATPase activity was measured as described in Ref. [9] by colorimetric determination of liberated inorganic phosphate [10]. The rate of phosphate liberation from ATP was measured in Medium S supplemented with 0.45 mM  $\text{CaCl}_2$  and 1  $\mu\text{M}$  A23187 at a protein concentration of 0.02 mg/ml at 25°C for 5 min [11], with and without glycerol or sucrose. SR vesicle suspensions were divided into two aliquots for instant spin labelling and parallel crystallization experiments, after a 24-h incubation period at 2°C in conjunction with electron microscopic measurements at this temperature. For negative staining the vesicle suspensions (1 mg of protein/ml) were placed on carbon-coated parlodion film and stained with freshly prepared 1% uranyl acetate (pH 4.3) at 2°C. Electron micrographs were recorded with a JEOL 100-B microscope at 80 kV accelerating voltage [11].

### 2.3. Spin labelling

$\text{Ca}^{2+}$ -ATPase was prelabelled with NEM on the fast reacting interfacial -SH groups (group I) at a labelling level of 1:1 mol/mol for 5 min [12]. Then, the intramembranous -SH groups (group II) were labelled with 5-MSL, in the presence of intercalated NEM, at a labelling level of < 1:1 mol/mol and of NEM for 40 min, and the unreacted NEM and spin labels were separated by centrifugation (Beckman 50Ti at 40 000 rpm) for 30 min. Spin-labelled stearic acid (16-SASL) was intercalated into SR membrane prior to the addition of polyols and incubated at ambient temperature (25°C) for 15 min before removing the non-intercalated spin probes by low-speed centrifugation.

### 2.4. ESR measurements

ESR spectra were recorded on a Bruker ECS 106 Series 9 GHz spectrometer equipped with a temperature regulation system based on pressured air gas flow. Spin labelled  $\text{Ca}^{2+}$ -ATPase rich vesicles were

packed in 1 mm I.D. capillaries by low-speed centrifugation. Temperature was measured by a fine-wire thermocouple located at the bottom of the microwave cavity within the Dewar insert. Conventional ( $V_1$ -display) and saturation transfer ( $V_2'$ -display) ESR spectra were recorded using 100 kHz and 50 kHz modulations using the recommended protocol for STESR measurements as described in Ref. [13]. The signal-to-noise ratio of the STESR spectra was improved by smoothing over a 5-point-window at low field, a 3-point-window in the centre, and a 7-point-window at high field in the case of line height ratio measurements. (It should be noted that the anisotropy in the three regions are 2.18, 1.01, and 3.70 mTesla, respectively.) Spectral amplitudes of the diagnostic points (L, L', H, and H'') of STESR spectra were evaluated as described in Ref. [14], and calibrations of STESR line height ratios ( $L'/L$  and  $H'/H$ ) and normalised STESR intensities of spin labelled haemoglobin were taken from Refs. [15,16].

### 3. Results

#### 3.1. Enzymatic activity measurements of $\text{Ca}^{2+}$ -ATPase

The enzymatic activity of  $\text{Ca}^{2+}$ -ATPase was sharply reduced on increasing the viscosity of the aqueous phase. However, as shown in Fig. 1, after the addition of sucrose or glycerol to the aqueous phase, the relative activity was reduced to different extent. As the viscosity was increased from 1.1 to 13.2 mPa · s ( $1 \times 10^{-3} \text{ Pa} \cdot \text{s} = 1 \times 10^{-2} \text{ Poise}$ ) by adding glycerol, the relative activity of the enzyme was reduced to 0.12, whereas on increasing the viscosity from 1.1 to 12.0 mPa · s by the addition of sucrose the relative activity was reduced to lesser extent, to 0.64. As to the analytical form of the viscosity induced relative activity reduction, in the case of sucrose the decline in relative enzymatic activity varied according to the inverse power law,  $\sim 1/\eta^b$ , with  $b = 0.21$ , typical for non-interacting solvents [17]. Glycerol, on the other hand, led to an exponential activity decay,  $\sim e^{-\beta\eta}$  with  $\beta = 0.17$ , indicating interaction between the solvent molecules and the extramembranous part of the polypeptide; a

more complete discussion for proteins of the plasma membrane is given in Ref. [18]. For the sake of comparison, the complementary forms of the viscosity dependence, namely exponential curve for sucrose and inverse power law for glycerol, are also shown in Fig. 1. Less acceptable fits were obtained with typical root-mean-square (R.M.S.) values of 97.2% versus 94.5% in the case of sucrose for fitting according to power law and exponential decay, and 89.2% versus 99.5% in the case of glycerol for fitting according to power law and exponential decay, respectively.

Crystalline arrays of  $\text{Ca}^{2+}$ -ATPase from native SR induced by vanadate were could be formed in the presence of glycerol, and essentially very similar arrays were obtained after the addition of glycerol to preformed 2D-crystals of the enzyme by negatively stained SR in agreement with previous results (EM pictures not shown, [4]). As demonstrated by EM neither the incorporation of spin labels [19] nor glycerol had any effect on 2D-crystal formation, at least using negative staining EM at low resolution.

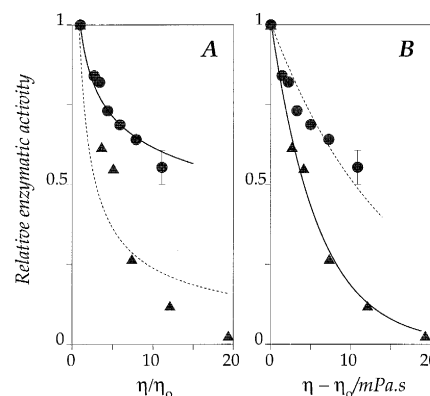


Fig. 1. The relative enzymatic activity of  $\text{Ca}^{2+}$ -ATPase as a function of the viscosity of the aqueous phase and best-fitting curves assuming reciprocal power law  $\sim 1/\eta^b$  (A) and exponential decay law  $\sim e^{-\beta\eta}$  (B) for calculation. Best fitting coefficient values were  $b = 0.21$  in the case of sucrose ( $\bullet$ ) and  $\beta = 0.17$  in the case of glycerol ( $\blacktriangle$ ); the root-mean-square error (R.M.S.) of fitting of inverse power law for sucrose (solid line in panel A) was 97.2%, while for glycerol the R.M.S. error was 99.5% (solid line in panel B). Best-fitting complementary curves in these cases (dashed lines) gave significantly worse fits. For sucrose, assuming the exponential decay law with  $\beta = 0.066$  an R.M.S. error of 94.5%, while for glycerol assuming inverse power law with  $b = 0.62$ , an R.M.S. error of 89.2% was obtained.

### 3.2. Conventional ESR spectra

On labelling  $\text{Ca}^{2+}$ -ATPase with spin-labelled maleimide (5-MSL), after brief prelabelling of the fast reacting interfacial -SH groups (group I) with NEM, a strongly immobilised line shape was obtained, indicating no significant segmental motion of the spin label when covalently bound (group II, [20]). It should be noted that spin labelling experiments were done at 20°C in a short time (< 1 h). The ubiquitous weakly immobilised component, which unlike the immobile component could be quenched by  $\text{Ni}^{2+}$  ions and, thus, assigned to covalently attached labels at the interface of the lipid bilayer or intercalated, but unbound spin labels in the intramembranous phase, was reduced to < 5% in a single washing step. The hyperfine splitting,  $2A_{\text{max}}$ , and the line widths at half-height,  $H_{\text{low}}$  and  $H_{\text{high}}$ , of the outer extrema (spectra not shown) were 68.0 Gauss, 3.0 Gauss, and 3.8 Gauss, respectively. It should be noted that the line width data depended on the labelling level and, thus, the  $\text{MSL}_{\text{bound}}/\text{Ca}^{2+}$ -ATPase molar ratio was kept constant at 0.75 mol/mol. The obtained spectral parameters agreed with previous results on label/protein stoichiometry experiments [12]. Since all spectra were close to the rigid limit line shape more quantitative experiments required STESR methods which have a time scale of  $10^{-6}$ – $10^{-4}$  s.

The intramembranous viscosity of the centre of the lipid bilayer was followed by spin-labelled stearic acid (16-SASL) intercalated prior to the addition of polyols to the aqueous phase. The rotational correlation time of C-16 spin labelled stearic acid was  $1.41 \pm 0.02 \times 10^{-9}$  s as measured by the line width method [21]. After the addition of sucrose or glycerol by increasing the aqueous viscosity of the extramembranous phase from 1.1 mPa·s to 12.0 or 20.5 mPa·s the correlation time remained unchanged:  $1.40 \times 10^{-9}$  s and  $1.38 \times 10^{-9}$  s, respectively.

### 3.3. Saturation transfer ESR spectra

A series of second-harmonic, 90° out-of-phase ( $V_2'$ ) STESR spectra of covalently labelled 5-MSL +  $\text{Ca}^{2+}$ -ATPase in Medium S supplemented with sucrose or glycerol of increasing viscosity is shown in Fig. 2. The signal-to-noise ratio of these spectra were

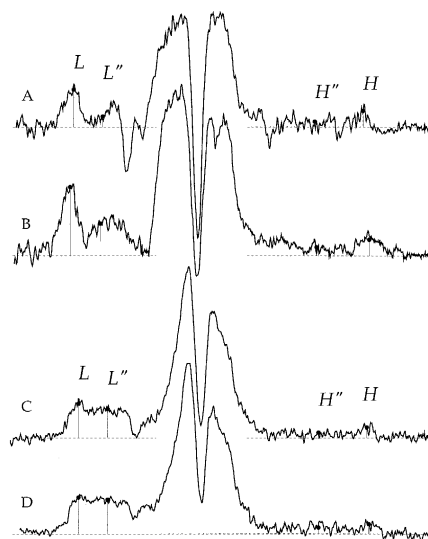


Fig. 2. Second harmonic, 90° out-of-phase absorption ( $V_2'$ ) STESR spectra of covalently-labelled sarcoplasmic reticulum vesicles at a labelling level of 5-MSL:  $\text{Ca}^{2+}$ -ATPase = 0.75 mol/mol and adding various amounts of sucrose or glycerol to Medium S and using the noise filter of 5-point-window method. (A) Spin-labelled SR vesicles in Medium S; (B) 50 w/v% sucrose and Medium S; (C) 52 w/v% glycerol and Medium S; (D) 64 w/v% glycerol and Medium S. Total scan width was 10 mTesla and the temperature was 293 K.

improved by smoothing over 5/3/7-point-window in the low-field, central, and high-field region and the signal-to-noise ratios were (at least) 8:1, 16:1, 3:1 and 18:1, 28:1, 8:1 in the untreated and smoothed spectra, respectively. On increasing the viscosity of the extramembranous phase progressive changes were observed in the line shapes of STESR spectra and, in particular, in the line heights in the diagnostic regions at low and high fields. All these spectra were obtained at the same labelling level ( $\text{MSL}_{\text{bound}}/\text{Ca}^{2+}$ -ATPase = 0.75 mol/mol) in order to control the effect of spin-spin interaction which was shown to influence selectively the normalised STESR intensity [12]. As the viscosity of the aqueous phase was increased from 1.1 to 12.0 mPa·s and 20.5 mPa·s by adding 50 w/v% sucrose and 74 w/v% glycerol at 20°C, respectively, the diagnostic line height ratios, which are sensitive to the rotational correlation time [22], were increased from  $L''/L = 0.29$  to 0.94 and  $H''/H = 0.30$  to 0.86 as expected for slowing molecular rotation.

The low-field ( $L''/L$ ) and high-field ( $H''/H$ ) line

height ratios were determined and compared to spin-labelled haemoglobin calibrations [15,16]. The difference between the correlation time values from low-field and high-field line height ratios were  $< 10$ –25% provided the signal-to-noise ratios allowed such comparisons. As a rule, the low-field line height ratio ( $L''/L$ ), after smoothing over a 5-point-window, was more affected by the overlapping mobile spectral component (Fig. 2). It should be noted that the experimental error in determining the STESR line height from the high-field region ( $H''/H$ ) was filtered by smoothing over a 7-point-window. The extramembranous height was estimated from average values obtained in low-field and high-field STESR measurements. The correlation time had an uncertainty of  $2.5 \times 10^{-6}$  s yielding a propagated error in the height data of  $5 \times 10^{-10}$  m. Qualitatively similar spectral changes were reported by Lewis and Thomas [19] and Napier et al. [23] for STESR spectra of covalently labelled  $\text{Ca}^{2+}$ -ATPase in two-dimensional  $\text{E}_2$  crystalline form.

The effective rotational correlation time of the protein depends on the orientation of labels to the membrane fixed co-ordinate axes [14]. However, this dependence is not influenced by the viscosity of the aqueous phase and so the ratio of the effective rotational correlation times in Medium S with and with-

out polyol is a suitable relative parameter which is not dependent on the orientation of spin labels. The ratio of the effective rotational correlation times from the STESR spectra of covalently labelled  $\text{Ca}^{2+}$ -ATPase suspended in sucrose or glycerol supplemented Medium S of different concentrations of polyols and normalised with the control, i.e.,  $(\tau_R - \tau_{R,m})/\tau_{R,m}$ , are given as a function of the measured viscosity in Fig. 3.  $\tau_R$  and  $\tau_{R,m}$  denote the rotational correlation time in the intramembrane phase with and without polyols in the aqueous phase, respectively. The effective correlation times for the native SR membranes in Medium S supplemented with glycerol were all significantly greater than those supplemented with sucrose at the same viscosity. The change in the rotational correlation time vs. viscosity curve was approximately linear in the case of sucrose, whereas it was linear in the semilogarithmic plot for glycerol.

#### 4. Discussion

$\text{Ca}^{2+}$ -ATPase of sarcoplasmic reticulum is one of the well-characterised integral membrane proteins for which a correlation has been found between molecular dynamics and enzymatic activity data [24,25]. The molecular structure of the enzyme was determined to 2.5 nm resolution and the height of the extramembranous segment was estimated to be  $\sim 6.0$  nm as measured by the combined application of frozen hydration EM of the intramembranous segment and negative staining EM of the extramembranous part [26]. Several data suggest that, although protein monomers retain many functions of the protein dimers which are held together by interacting extramembranous parts, the functional unit of SR calcium pump is a dimer [27]. The connection of neighbouring extramembranous domains has a decisive role in forming protein dimers and 2D protein crystals [11]. According to three-dimensional reconstruction protein dimers are connected by peptide-bridges formed at a height of 4.2 nm above the membrane surface, and in two-dimensional  $\text{E}_2$  protein crystals an additional peptide-bridge was observed at the height of 1.6 nm above the interfacial surface [26].

In previous reports of multilamellar crystals of detergent solubilised  $\text{Ca}^{2+}$ -ATPase it was suggested

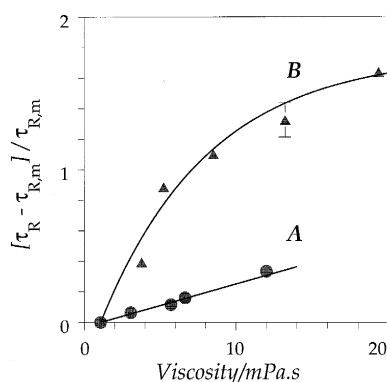


Fig. 3. The normalised effective correlation time increase of covalently labelled  $\text{Ca}^{2+}$ -ATPase as a function of aqueous phase viscosity after the addition of sucrose (A,  $\bullet$ ) or glycerol (B,  $\blacktriangle$ ). The correlation times were determined from the combined application of the low-field ( $L''/L$ ) and high-field ( $H''/H$ ) line height ratios of STESR spectra. The measured points for sucrose are shown together with a best-fitting straight line (solid line) following Eq. (1) in the interval of  $\eta = 0$ –12 mPa·s and for glycerol with a logarithmic curve in the interval of  $\eta = 0$ –20 mPa·s.

that glycerol has an inhibitory effect on in-plane nucleation, but crystal fusion after nucleation was facilitated [28–30]. As known from crystallization experiments, the presence of glycerol does not influence the formation of peptide-bridges which are essential in building-up of protein crystals [26,31]. Implicit to these crystallization experiments is that the molecular dimensions are not greatly perturbed by the presence of glycerol molecules; the effect of sucrose on crystallization is discussed later.

The dependence of the rotational correlation time increase on aqueous viscosity,  $\eta$ , is given according to Esmann et al. [2] by

$$\tau_R - \tau_{R,m} = \frac{2\eta}{3kT} \sum_{i=1}^2 \frac{V_i}{F_i} \quad (1)$$

where  $V_i$  denote the volumes of enzyme in the matrix and intracellular sides of the sarcoplasmic reticulum membrane ( $i = 1, 2$ ) and  $F_i$ 's are the respective ellipticity factors [8]; other parameters, as usual,  $k$  and  $T$  denote Boltzmann's constant and temperature, respectively. The effective rotational correlation time, thus, depends primarily on the intramembranous viscosity  $\eta_m$  [1], the ellipticity contour  $F_i$  [31] and the orientation of the spin label [8,14], as discussed below.

The leading term in the rotational correlation time  $\tau_R$  is the contribution to the correlation time due to the intramembranous part  $\tau_{R,m}$  which varies with the intramembranous viscosity in the range of  $\eta = 200$ – $500$  mPa · s (a value of  $\eta = 370$  mPa · s is used in [32]) and the contribution of the extramembranous part in the aqueous phase (1.1 mPa · s) is usually neglected to first approximation, i.e.,  $\tau_R \approx \tau_{R,m}$ . Eq. (1) is based on two assumptions: namely, (1) the torque due to the intramembranous and extramembranous parts of the enzyme consists of additive, almost collinear, vectors [33] and, hence, the increase in rotational correlation time is linearly proportional to the viscosity of the aqueous phase, and (2) the extramembranous and intramembranous segments are rigidly connected. This assumption is certainly applicable in the case of  $\text{Ca}^{2+}$ -ATPase according to recent three-dimensional modelling [26,34].

A simplifying assumption, in agreement with three-dimensional reconstruction of the enzyme in  $E_1$  and  $E_2$  forms, is that the ellipticity factor is uniform across the various parts in different viscous phases.

According to morphological data the ellipticity factor is 0.87 and will only change by the formation of two-dimensional aggregation [12]. The 'pear-shaped' molecule has no large extensions either in the intramembranous or extramembranous parts, suggesting an evenly round mobile contour [35].

Strictly speaking the effective correlation time is related to the diffusion tensor and the orientation of NO-group, as discussed in Ref. [14]. By paramagnetic quenching of transition ions, like nickel soluble in the aqueous phase, it has been shown that the spin label has covalently been attached to -SH groups in the intramembranous part of the enzyme molecule prior to the addition of polyols and it is assumed that the orientation of spin label is not modified by the aqueous viscosity. In this case the ratio of the correlation times prior to and after the addition of viscous polyols is not dependent on the orientation of the label.

For quantitative evaluation an experimental parameter is introduced

$$\frac{\tau_R - \tau_{R,m}}{\tau_{R,m}} = \frac{\eta V_1}{\eta_m V_m} \quad (2)$$

normalising the measured correlation time increase ( $\tau_R - \tau_{R,m}$ ) with that due to the intramembranous contribution  $\tau_{R,m}$ . It should be noted that the ratio  $(\tau_R - \tau_{R,m})/\tau_{R,m}$  is dependent on the ratios of viscosity of the different phases ( $\eta$  and  $\eta_m$ ) and the respective volume parts of the enzyme ( $V$  and  $V_m$ ) but not dependent on the ellipticity factor and the orientation of the spin labels. The protruding part of the enzyme, as a rotating body, is taken as a cylinder of elliptic cross-section; denoting the semi-axes of the ellipsis by  $a$  and  $b$ , and its height by  $h$  for its volume  $V = Ah = ab\pi h$  is obtained [36]. The protrusion on the luminal side is neglected ( $V_2 \approx 0$ ) with respect to that on the cytosolic side ( $V_1$ ) since the location of  $\text{Ca}^{2+}$ -ATPase in the two aqueous phases is fairly asymmetric [24,26,34].  $\text{Ca}^{2+}$ -ATPase, like many proteins, has a discontinuous contour at the membrane/aqueous phase interface: the areas of compact intramembranous ( $A_m$ ) and more extensive extramembranous ( $A$ ) segments change markedly [34,37]. The ratio of two adjoining segments,  $A/A_m$ , can vary from 1, i.e., no change at the interface, to 4, corresponding to a twofold size increase. According

to low-resolution diffraction measurements on two-dimensional  $E_2$  crystals of  $Ca^{2+}$ -ATPase the ratio of the cross-sections in the extramembranous and intramembranous segments is  $A/A_m \sim 3$  [34,35,37]. In this approximation the ratio of the extramembranous and transmembrane segments is given by

$$\frac{\tau_R - \tau_{R,m}}{\tau_{R,m}} = \frac{A}{A_m \eta_m} \eta \frac{h}{h_m} \quad (3)$$

and so the normalised correlation time increase will be proportional to the viscosity of the aqueous phase  $\eta$  and the height of the extramembranous part  $h$ .

The viscosity dependence is determined, according to Eq. (2), by the viscosity of the intramembranous phase and the measured values for various membranes specify a range of 200–500 mPa · s [32]. At the lower and upper limits, assuming equal heights for the intramembranous and extramembranous segments  $h_m = h$ , for the slope values of the  $(\tau_R - \tau_{R,m})/\tau_{R,m}$  vs.  $\eta$  curves  $0.015 \text{ (mPa} \cdot \text{s)}^{-1}$  and  $0.006 \text{ (mPa} \cdot \text{s)}^{-1}$  are expected, respectively. The measured slope of the  $(\tau_R - \tau_{R,m})/\tau_{R,m}$  vs.  $\eta$  curve was  $0.0235(5) \text{ (mPa} \cdot \text{s)}^{-1}$  on increasing the viscosity of the aqueous phase by the addition of sucrose (Fig. 3). Thus, the ratio of the two segments is related to the membrane thickness as  $h/h_m \sim 1.6$  and  $3.9$  at the lower and upper limits of intramembranous viscosity ranges, respectively. Assuming a membrane thickness of  $h_m = 4.5 \text{ nm}$ , this measurement gives for the height of the extramembranous segment  $h = 6.8 \text{ nm}$  and  $17 \text{ nm}$  at the lower and upper limits of the viscosity range, respectively. Accordingly 82–92% of the volume of the volume of  $Ca^{2+}$ -ATPase protein is external to the sarcoplasmic reticulum. The value at the lower limit of intramembranous viscosity range is in good agreement with previous data obtained from low-resolution diffraction and three-dimensional molecular reconstruction estimates [27]. It should be noted that the calculated height of the extramembranous segment depends on the value of intramembranous viscosity and, thus, fluidity modulation due to temperature changes or alteration in the concentration of membrane-soluble drugs could modify the size of protruding segments.

There are two independent lines of indications that glycerol and sucrose exert qualitatively different alterations on interacting with  $Ca^{2+}$ -ATPase. In the

case of these polyols, although both inhibited enzymatic activity, qualitatively different viscosity dependencies were observed. Large concentrations ( $> 0.5 \text{ M}$ ) of sucrose have prevented the formation of decavanadate induced  $E_2$  crystals, whereas 40 w/v% glycerol even improved the self-association of the solubilised enzyme [28]. The simple linear dependence on viscosity predicted by Eq. (1), which has given a consistent explanation of correlation time and enzymatic activity data for sucrose, does not give an acceptable fit for glycerol (cf. Figs. 1 and 3). In addition, glycerol is a generally used polyol to facilitate the polymerisation of crystal patterns of solubilised  $Ca^{2+}$ -ATPase [28,38], whereas sucrose was a polyol supplement which at low concentrations (up to  $0.4 \text{ M}$ ) had no effect on two-dimensional (2D) crystal formation in native SR, while at high concentrations ( $0.5$ – $1 \text{ M}$ ) it abolished the process [39].

The correlation time data evaluated from STESR line height parameters display similar correlation time increases on adding glycerol for varying the viscosity, but the observed changes were both quantitatively and qualitatively rather different from that measured after the addition of sucrose. The effective correlation times of covalently labelled  $Ca^{2+}$ -ATPase in glycerol suspensions are much greater than those in sucrose suspension of the same viscosity, suggesting the formation of larger protein aggregates. Alternatively, the height of the extramembranous fraction ought to be increased by a factor of  $\sim 5$  on expense of the intramembranous fraction; this is in contradiction with the balance of hydrophobic forces. It should be noted that the addition of glycerol, which leads to the formation of such aggregates, could serve as an effective enzyme inhibitor in agreement with the steeply declining activity data. As another mechanism, namely the effect of dehydration due to solute/protein interaction, is discussed by Esmann et al. [2].

In conclusion, the ATP hydrolysing activity of the enzyme decreased differently on adding sucrose and glycerol. The effective rotational correlation time of the protein increased linearly with the viscosity of the sucrose containing medium giving an extramembranous height of  $6.8 \text{ nm}$ . Glycerol, as indicated by the greater changes in rotational mobility and non-linear viscosity dependence, led to the formation of larger aggregates.

## Acknowledgements

M.T. gratefully expresses her thanks for a doctoral fellowship to Ministry of Education. The usage of rotating disc viscometer is gratefully acknowledged to Professor I. Dékány (University of Szeged). This work was supported by grants from Hungarian National Science Foundation (OTKA T12747/1994 to A.B.; OTKA T6277/1993 to L.D.; OTKA T13257/1994 to L.I.H.).

## References

- [1] Saffman, P.G. and Delbrück, M. (1975) *Proc. Natl. Acad. Sci. USA* 72, 3111–3113.
- [2] Esmann, M., Hideg, K. and Marsh, D. (1994) *Biochemistry* 33, 3693–3697.
- [3] Sandermann, H. (1978) *Biochim. Biophys. Acta* 515, 209–237.
- [4] Dux, L. (1993) *Rev. Physiol. Biochem. Pharmacol.* 122, 2599–2603, Springer, Berlin.
- [5] Sousa, R. (1995) *Acta Cryst. D51*, 271–277.
- [6] Thomas, D.D., Dalton, L.R. and Hyde, J.S. (1976) *J. Chem. Phys.* 65, 3006–3024.
- [7] Berliner, L.J., ed. (1979) *Spin Labeling II: Theory and Applications*, Academic Press, New York.
- [8] Marsh, D. and Horváth, L.I. (1989) in *Advanced EPR in Biology and Biochemistry* (A.J. Hoff, ed.), pp. 707–772, Elsevier, Amsterdam.
- [9] Nakamura, H., Jilka, R.L., Boland, R. and Martonosi, A.N. (1976) *J. Biol. Chem.* 251, 5414–5423.
- [10] Eibl, H. and Lands, W.E.M. (1969) *Anal. Biochem.* 30, 51–57.
- [11] Dux, L. and Martonosi, A.N. (1983) *J. Biol. Chem.* 258, 2599–2603.
- [12] Horváth, L.I., Dux, L., Hankovszky, H.O., Hideg, K. and Marsh, D. (1990) *Biophys. J.* 58, 231–241.
- [13] Hemminga, M.A., De Jager, P.A., Marsh, D. and Fajer, P. (1984) *J. Magn. Reson.* 59, 160–163.
- [14] Robinson, B.H. and Dalton, L.R. (1980) *J. Chem. Phys.* 72, 1312–1324.
- [15] Horváth, L.I. and Marsh, D., (1988) *J. Magn. Reson.* 80, 314–317.
- [16] Marsh, D. and Horváth, L.I. (1992) *J. Magn. Reson.* 99, 323–331.
- [17] Kramers, H.A. (1940) *Physica* 7, 284–304.
- [18] Bérczi, A. and Moller, I.M. (1993) *Physiol. Plantarum* 89, 409–415.
- [19] Lewis, S. and Thomas, D.D. (1986) *Biochemistry* 25, 4615–4621.
- [20] Hidalgo, C. and Thomas, D.D. (1977) *Biochem. Biophys. Res. Commun.* 78, 1175–1182.
- [21] Schreier, S., Polnaszek, C.F. and Smith, I.C.P. (1978) *Biochem. Biophys. Acta* 515, 375–436.
- [22] Squier, T.C. and Thomas, D.D. (1986) *Biophys. J.* 49, 921–935.
- [23] Napier, R.M., East, J.M. and Lee, A.G. (1987) *Biochim. Biophys. Acta* 903, 365–375.
- [24] MacLennan, D.H., Brandl, Ch.J., Korczak, B. and Green, N.M. (1985) *Nature* 316, 696–700.
- [25] Martonosi, A.N. and Beeler, T.J. (1983) in *Handbook of Physiology, Skeletal Muscle* (Peachey, L.D., Adrian, R.H. and Geiger, S.R., eds.), pp. 417–485, American Physiological Society, Bethesda.
- [26] Taylor, K.A., Dux, L. and Martonosi, A. (1986) *J. Mol. Biol.* 187, 417–427.
- [27] Andersen, J.P. (1989) *Biochim. Biophys. Acta* 988, 47–76.
- [28] Varga, S., Taylor, K.A. and Martonosi, A. (1991) *Biochim. Biophys. Acta* 1070, 374–386.
- [29] Shi, D., Hsiung, H.-H., Pace, R.C. and Stokes, D.L. (1995) *Biophys. J.* 68, 1152–1162.
- [30] Cheong, G.-W., Young, H.S., Ogawa, H., Toyosima, C. and Stokes, D.L. (1996) *Biophys. J.* 70, 1689–1699.
- [31] Napolitano, C.A., Cooke, P., Segalman, K. and Herbet, L. (1983) *Biophys. J.* 42, 119–125.
- [32] Cherry, R.J. and Godfrey, R.E. (1981) *Biophys. J.* 36, 257–276.
- [33] Feynman, R.P., Leighton, R.B. and Sands, M. (1963) *The Feynman Lecture on Physics*, Chpt 20, Addison-Wesley, Reading, MA, USA.
- [34] Toyoshima, Ch., Sasabe, H. and Stokes, D.L. (1993) *Nature* 362, 469–471.
- [35] Taylor, K.A., Ho, M.H. and Martonosi, A. (1986) *Ann. Rev. NY Acad. Sci.* 483, 31–43.
- [36] Jähnig, F. (1986) *Eur. J. Biophys.* 14, 63–64.
- [37] Blasie, J.K., Herbet, L.G., Pascolini, D., Skita, V., Pierce, D.H. and Scarpa, A. (1985) *Biophys. J.* 48, 9–18.
- [38] Varga, S., Mullner, N., Pikula, S., Papp, S., Varga, K. and Martonosi, A. (1986) *J. Biol. Chem.* 261, 13943–1396.
- [39] Dux, L. and Martonosi, A. (1983) *J. Biol. Chem.* 258, 10111–10115.